Nuclear Instruments and Methods in Physics Research A313 (1992) 126–134
North-Holland

NUCLEAR
INSTRUMENTS
& METHODS
IN PHYSICS
RESEARCH
Section A

Intercalibration of the ZEUS high resolution and backing calorimeters

H. Abramowicz [a,1], H. Czyrkowski [b], A. Derlicki [b], T.Z. Kowalski [c], M. Krzyżanowski [b], I. Kudla [b], W. Kuśmierz [b], R.J. Nowak [b], J.M. Pawlak [b], A. Rajca [b], A. Stopczyński [b], R. Walczak [b] and A.F. Żarnecki [b]

[a] *Deutsches Elektronen-Synchrotron, DESY, Hamburg, Germany*
[b] *Institute of Experimental Physics, Warsaw University *, Poland*
[c] *Institute of Physics and Nuclear Techniques, Academy of Mining and Metallurgy, Cracow, Poland*

Received 23 August 1991

We have studied the combined performance of two calorimeters, the high resolution uranium–scintillator prototype of the ZEUS forward calorimeter (FCAL), followed by a prototype of the coarser ZEUS backing calorimeter (BAC), made out of thick iron plates interleaved with planes of aluminium proportional chambers. The test results, obtained in an exposure of the calorimeter system to a hadron test beam at the CERN SPS, show that the backing calorimeter does fulfil its role of recognizing the energy leaking out of the FCAL calorimeter. The measurement of this energy is feasible, if an appropriate calibration of the BAC calorimeter is performed.

1. Introduction

The forthcoming new high energy accelerator facilities have renewed the interest in studying new solutions for calorimetric energy measurements. An interesting solution for optimizing energy measurements in terms of resolution and cost has been put forward by two experiments, ZEUS [1] and H1 [2], aimed at studying high energy electron–proton scattering at the electron–proton storage ring HERA, currently being built at DESY, Hamburg. The external iron yoke and muon absorber, surrounding the main components of the detector, is instrumented to allow an energy measurement for showers leaking out of the central, high resolution calorimeter.

In the case of the ZEUS experiment, the main calorimeter (CAL) is a fine grained sampling calorimeter made of depleted uranium and scintillator, 4 to 7 λ_{int} deep [1], followed by an iron backing calorimeter (BAC), made out of 8 to 11, 7.3 cm thick Fe plates interleaved with aluminium proportional tubes. As part of the preparation for the experiment, a test setup was built, consisting of CAL and BAC prototypes, in a configuration compatible with the forward part of the ZEUS detector [1]. This setup has been exposed to the X5 test beam at the CERN SPS, where the beam momentum could be varied between 10 and 100 GeV/c. In this paper we would like to concentrate on results obtained for the combined FCAL (short for *f*orward part of the uranium *cal*orimeter) and BAC prototypes. The results on the performance of FCAL and BAC as stand-alone units are presented elsewhere [3,4].

2. Experimental setup

2.1. Beam

The experimental setup in the beam line is shown in fig. 1. The X5 beam at the CERN SPS provides hadrons, electrons and muons with momenta ranging from 10 to 100 GeV/c. For the present analysis only hadron events were selected. A set of scintillation counters, B_1 to B_4, was used as a trigger. Two Cherenkov counters, $\check{C}_1$ and $\check{C}_2$, filled with helium and nitrogen, respectively, were used for electron–hadron discrimination. In addition, a set of drift chambers, DC_1 and DC_2, was used to reject halo particles in the off-line analysis. The data used for this analysis were collected at energies of 50, 75 and 100 GeV.

[1] Alexander von Humboldt Fellow, on leave of absence from Institute of Experimental Physics, Warsaw University, Poland.

* Partly supported by Ministry of National Education, Poland.

2.2. Data

The total sample consists of 80000 events, with 55000 events collected at 100 GeV, 14000 at 75 GeV and 11000 at 50 GeV. In order to increase the statistics of events with high energy deposits in the BAC prototype, some data were taken with an additional trigger requiring a deposit of more than 4 GeV in the BAC.

2.3. FCAL calorimeter

The FCAL prototype was built of 4 modules, each consisting of 4 towers of 20×20 cm^2. Each module is divided longitudinally into one electromagnetic part (EMC), $0.96\lambda_{int}$ deep, and two hadronic parts (HAC1 and HAC2), $3.09\lambda_{int}$ each. The total depth of the calorimeter, with lateral dimension 80×80 cm^2, was equivalent to $7.1\lambda_{int}$. The active part of the calorimeter is followed by a nonactive layer. This nonactive layer consists of mechanical supports, a layer of photomultipliers with their shieldings, and cables and was estimated to be equivalent to about 15 cm of iron. The main parameters of the FCAL prototype are summarized in table 1. The calibration of the FCAL towers was based on lateral electron and muon scans and was monitored by regular measurements of the signal from the uranium radioactivity. The energy resolution obtained for fully contained hadronic showers is about $35\%/\sqrt{E}$. For details the interested reader is referred to ref. [3].

Table 1
Main parameters of the FCAL prototype

	FCAL calorimeter	
	EMC section	HAC1, HAC2
Absorber material	depleted uranium (DU)	
Absorber cladding	stainless steel	
Readout material	SCSN-38 scintillator (SCI)	
DU thickness [mm]	3.3	3.3
Cladding thickness [mm]	0.2	0.4
SCI thickness [mm]	2.6	2.6
Number of layers	25	80
Section length [cm]	24 cm $26 X_0$ $0.96\lambda_{int}$	64 cm $85 X_0$ $3.09\lambda_{int}$
Transverse segmentation [cm^2]	5×20	20×20
Total depth [cm]	152 $196 X_0$ $7.1\lambda_{int}$	
Total cross-section [cm^2]	80×80	
Optical readout	WLS + light guides + photomultipliers	

2.4. BAC calorimeter

The prototype of BAC was made out of 11 iron plates of 2×2 m^2, 7.3 cm thick, interleaved with 10 layers of aluminium proportional chambers, 12 in each layer. Each chamber contains 8 cells, 1.1×1.5 cm^2, with a 50 μm gold-plated tungsten wire in the center of each call. A gas mixture of 87% Ar + 13% CO_2 was used, and the high voltage was set at 1.785 kV. Signals both from the wires and from the cathode planes (so-called pads) could be used to determine the deposited energy. The pad towers are obtained by summing in depth signals from the 50×50 cm^2 cathode pads. The wire towers are obtained by summing up in depth the 53×200 cm^2 wire planes. The signals from the towers (12 pad towers and 3 wire towers), after shaping, are read by an 8-bit Flash-ADC, working with a 96 ns clock. The results presented in this paper were obtained by using signals from the wire towers only. With this readout the energy resolution obtained for hadrons was about $120\%/\sqrt{E}$. The details of the readout, the signal definition and the calibration procedure of the BAC prototype can be found in ref. [4].

2.5. Veto calorimeter

In addition to the FCAL and BAC prototypes, a third calorimeter was used to monitor energy leakage

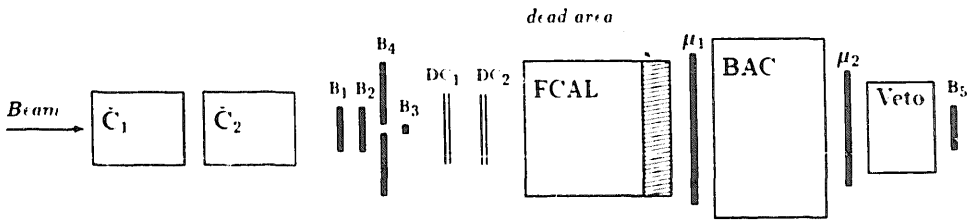

Fig. 1. Experimental setup (not to scale).

Table 2
Main parameters of the BAC prototype and the veto calorimeter

	BAC prototype	Veto calorimeter
Absorber material	iron	
Readout medium	aluminium proportional chambers	
Gas mixture	87% Ar + 13% CO_2	
Absorber thickness [cm]	7.3	5.0
Number of absorber layers	11	9
Number of chamber planes	10	8
Total length [cm]	115	73
	46 X_0	26 X_0
	4.9 λ_{int}	2.8 λ_{int}
Total crosssection [m^2]	2 × 1.6	0.96 × 0.88
Readout	anode wires	cathode planes

out of the whole calorimeter system, and to reject muon events. This veto calorimeter was made of 9 iron plates of 88 × 96 cm^2, 5 cm thick, interleaved with 8 layers of aluminium proportional tubes, the same as for BAC. Signals from pads were summed in depth in three towers and read out by the 2249A LeCroy ADC. In the analysis, only those events were used for which the signal in the veto calorimeter was smaller than 0.05 GeV, equivalent to about $\frac{1}{20}$ of the mean muon signal. At 100 GeV this requirement rejects about 2.4% of hadronic events. In table 2 the main parameters of the veto calorimeter are compared with those of the BAC calorimeter.

2.6. Muon chambers

Two planes of the aluminium proportional chambers (same type as for BAC and the veto calorimeter) were also used as muon chambers. They were placed in front of and behind BAC (see fig. 1), as in the ZEUS detector [1]. For both planes, only the pad signals were read out. The first plane, μ_1, can be used to correct for losses in the nonactive material behind the FCAL prototype. The second one, μ_2, was used to improve the efficiency of the leakage veto. The percentage of leaking events rejected, including the muon chamber information, increases to 3.2% at 100 GeV. Those events were removed from the sample used for further analysis.

3. Performance of the combined FCAL and BAC calorimeters

The depth of the FCAL prototype is such that for 90% of showers initiated by single hadrons with an energy of about 100 GeV, at least 95% of the energy is contained within the calorimeter [1,5]. The contribution of events with energy leaking from FCAL can be substantially suppressed by applying cuts on the signal in the veto system consisting of the μ_1 muon chamber located between FCAL and BAC and BAC itself. A cut of 0.5 GeV on the signal in the veto system, corresponding to less than one minimum ionizing particle, rejects at 100 GeV about 30% of all the events. As can be seen from fig. 2, where the total energy in the FCAL is plotted against the fraction of energy deposited in HAC2, even the 0.5 GeV cut does not reject all the noncontained events, due to the nonactive layer between FCAL and BAC. For events in which most of the energy is deposited in the HAC2 section of FCAL, the calorimeter response decreases. The measured energy for these events can be corrected, by taking into account the correlation between the total energy meausured in FCAL, E_{DU}, and the fraction of energy $r = E_{HAC2}/E_{DU}$ deposited in HAC2 (see fig. 2).

The dependence of the most probable E_{DU} as a function of r is shown in fig. 3. For the sake of completeness, the fraction of events in a given r bin is shown in fig. 4. The effect of missing energy for events with large energy deposits in HAC2 has also been observed in 50 and 75 GeV hadron runs. This is shown in fig. 5, where the correction to the total energy measured in FCAL is plotted against r, for the 50, 75 and 100 GeV runs. For $r \leq 25\%$, the correction is compatible with zero. For $r > 25\%$ the correction does not depend on the beam energy and can be well approximated by a linear function. In further analysis,

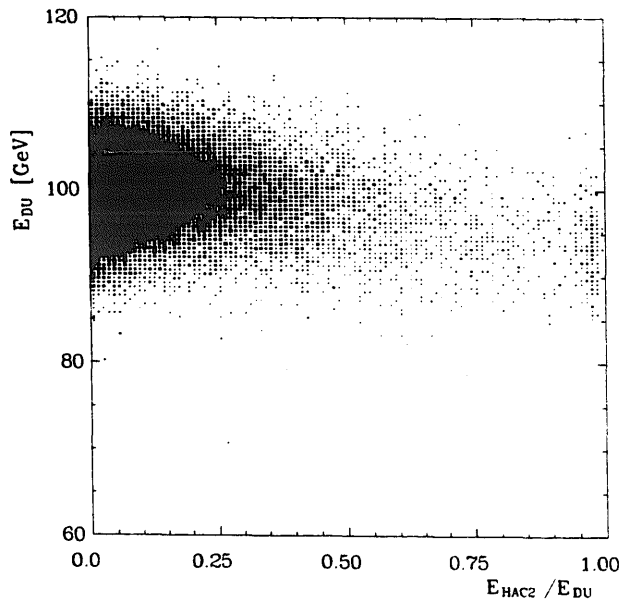

Fig. 2. Total energy deposited in the FCAL modules, E_{DU}, as a function of the fraction of E_{DU} measured in the HAC2 module, for 100 GeV hadron beam, for events with no signal in the veto system (μ_1 and BAC).

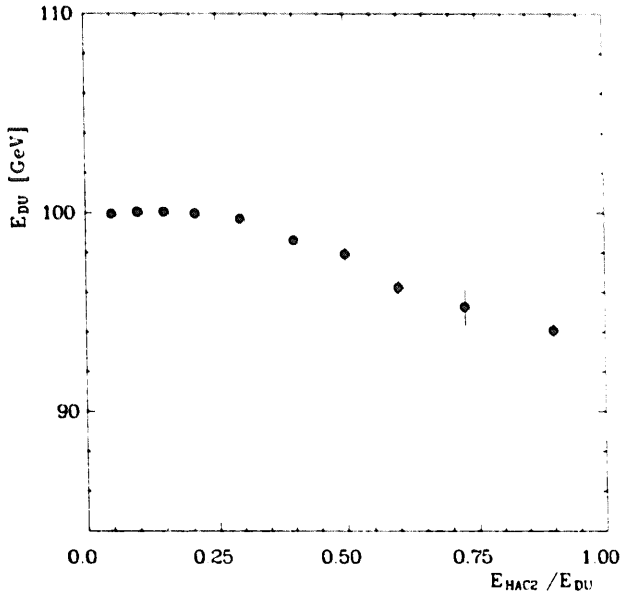

Fig. 3. Dependence of the most probable value of the total energy distribution as measured in the FCAL prototype, E_{DU}, on the value of the fraction of E_{DU} measured in HAC2, for 100 GeV hadron beam, for events with no signal in the veto system (μ_1 and BAC).

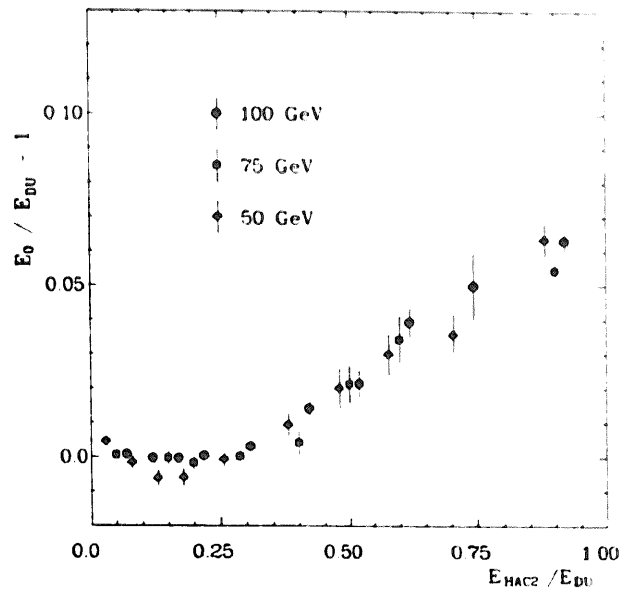

Fig. 5. The fractional correction to the energy measured in the FCAL prototype, E_{DU}, as a function of the fraction of E_{DU} measured in HAC2, for hadron energy E_0 = 50, 75 and 100 GeV, as indicated in the plot, for events with no signal in the veto system (μ_1 and BAC).

the correction determined from the sample of events with no leakage to the veto system is applied to all the events of the sample, depending on their r value.

The energy distribution of the 100 GeV hadrons, for events with no leakage into the veto system, is shown in fig. 6, after applying the correction described above. The distribution is overlayed with a Gaussian fit which gives a resolution of $38\%/\sqrt{E}$ for 100 GeV hadrons. This number is not in contradiction with the $35\%/\sqrt{E}$ determined in previous tests [3], since it is obtained without correcting for the momentum spread of the beam and the electronic noise. During the course of the runs discussed in this paper, the momen-

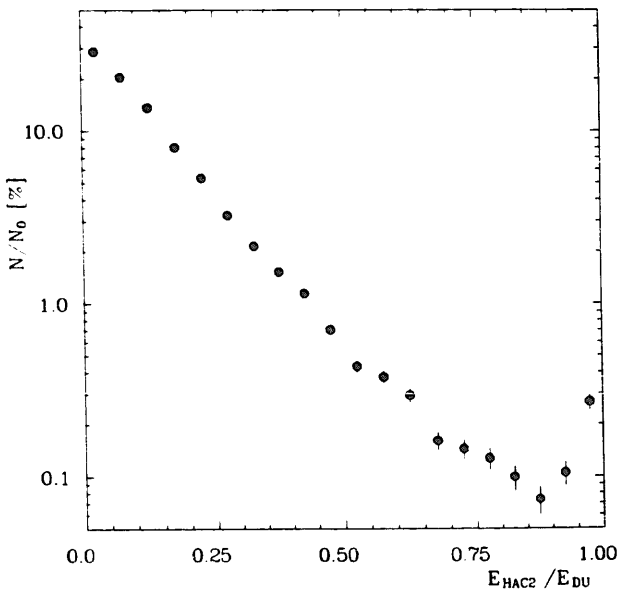

Fig. 4. The percentage of events with a given fraction of E_{DU} measured in HAC2 as a function of this fraction, for 100 GeV hadron beam, for events with no signal in the veto system (μ_1 and BAC).

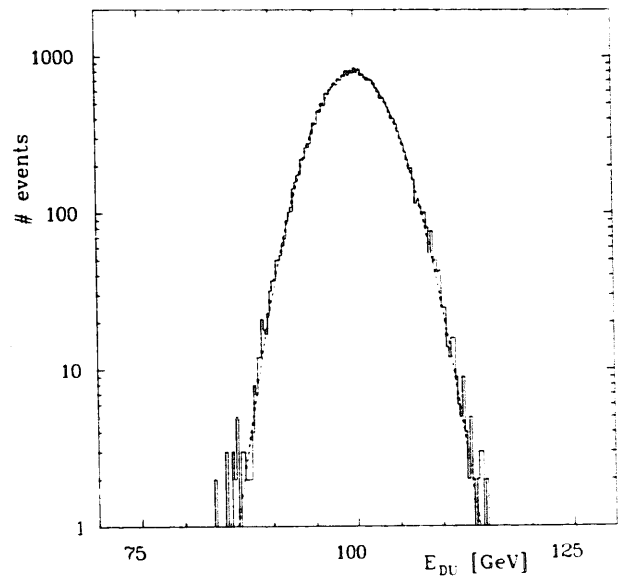

Fig. 6. Energy distribution for 100 GeV hadron events fully contained in the FCAL prototype (as determined by the veto system), after correction applied for the energy missing in HAC2. Overlayed (dashed line) is the result of a Gaussian fit to this distribution.

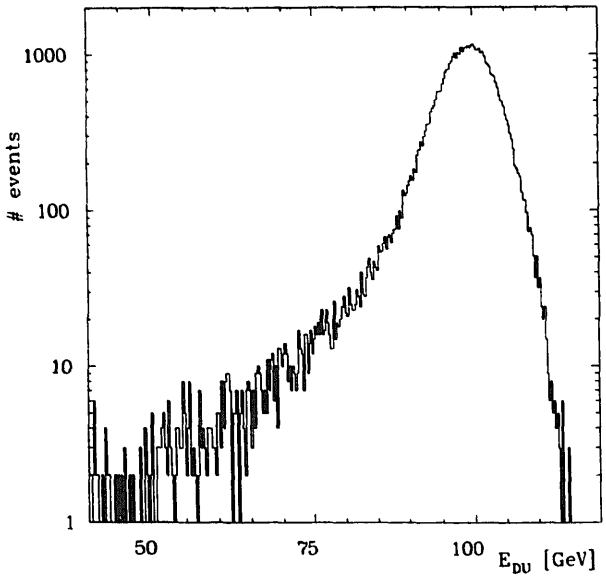

Fig. 7. Distribution of the energy measured in the FCAL prototype alone, for 100 GeV hadrons, with no cut longitudinal energy leakage.

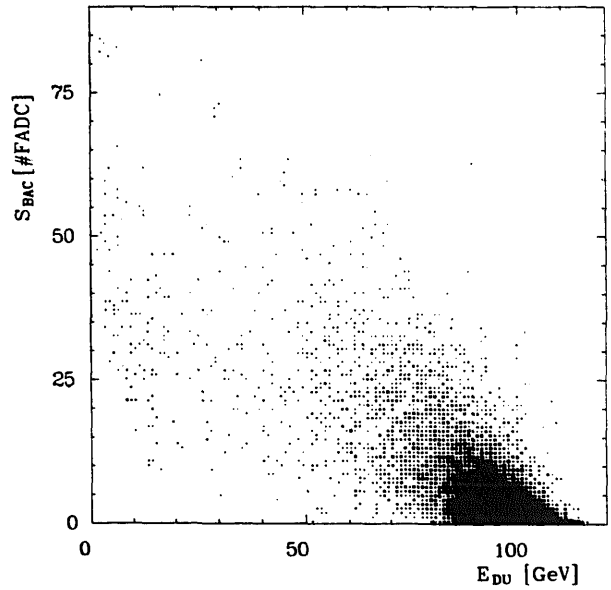

Fig. 8. Correlation between the BAC signal and the energy measured in FCAL, for a 100 GeV hadron beam.

tum spread of the beam (estimated to be about 1.5%) was not measured on an event-by-event basis, but its influence on the intercalibration of FCAL and BAC is negligible.

3.1. Intercalibration of the FCAL and BAC calorimeters

The intercalibration between FCAL and BAC was studied only for those events which do not leak out into the small veto calorimeter. The distribution of energy measured in FCAL, for 100 GeV hadrons, for all events, including those leaking into BAC, is shown in fig. 7. The distribution is asymmetric, with a long tail of events with significantly underestimated total energy. For over 5% of the events the meausured energy is below 3σ from the most probable value. However, there is a clear correlation between signals from the FCAL and BAC calorimeters as shown in fig. 8, indicating that the backing calorimeter is sensitive to the amount of energy leaking from FCAL. Therefore BAC can be used not only to select a sample of events fully contained in the uranium calorimeter, but also to measure the leaking energy.

The measurement of the energy leakage can be improved by making use of the signal from the first plane of muon chambers, placed between the FCAL and BAC calorimeters. This signal carries an additional information about the longitudinal shower profile, reflecting the number of charged particles entering the BAC calorimeter. The response distribution for the muon chambers, for 100 GeV hadron events, is shown in fig. 9. A single particle peak is clearly separated from the pedestal (reflecting showers fully contained in the FCAL calorimeter), and a long tail of events with many charged particles escaping from the FCAL is observed. About 30% of hadronic showers leak out of the uranium calorimeter, with a mean multiplicity of 3.5 charged particles entering the BAC calorimeter (the mean muon response is about 75 ADC channels).

The calibration of BAC and of the first layer of muon chambers, μ_1, is determined by optimizing the resolution of the energy distribution obtained by adding

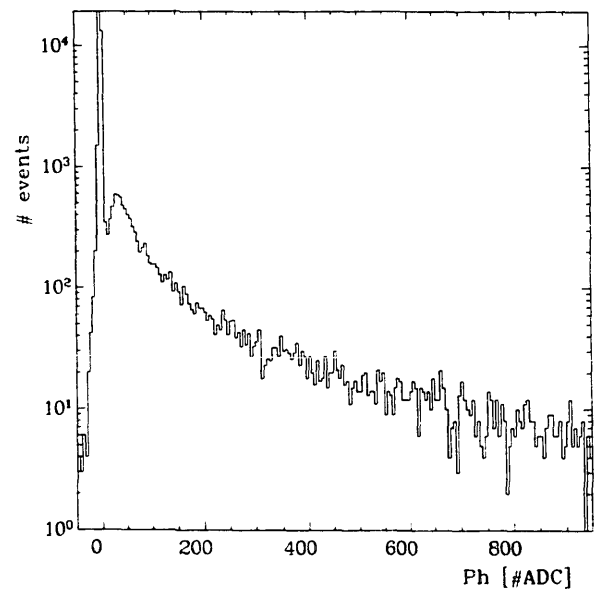

Fig. 9. The response distribution of the first layer of muon chambers, μ_1, placed between the FCAL and BAC prototypes, for 100 GeV hadrons.

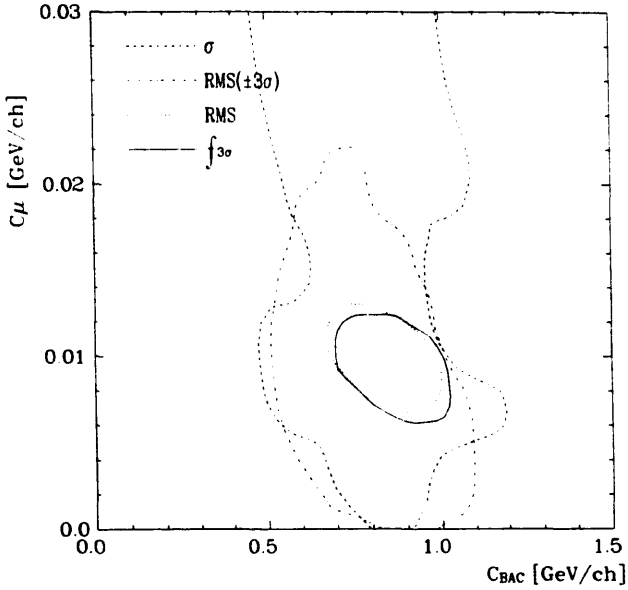

Fig. 10. One standard deviation contours for the calibration constants of the BAC prototype (c_{BAC}) and the μ_1 muon chamber (c_μ), as obtained for 100 GeV events from optimization of four different resolution estimators, as indicated in the plot.

the FCAL response to the BAC and muon chambers response weighted appropriately:

$$E = E_{DU} + c_{BAC} S_{BAC} + c_\mu S_\mu ,$$

where c_{BAC}, c_μ are the calibration constants and S_{BAC}, S_μ are the signals measured in BAC and the muon chambers respectively.

However, the energy distribution obtained by adding the response of the two different calorimeters tends to develop non-Gaussian tails. In that case the optimum resolution is not uniquely defined. In order to describe the response distribution we have determined the position of the maximum, by fitting a Gaussian function in a limited range around the maximum, and the FWHM, by fitting separately the two slopes of the distribution. We have tried to use the following quantities as estimators for the resolution:

- the width of the distribution determined from FWHM, $\sigma = \mathrm{FWHM}/\sqrt{2 \ln 2}$;
- the rms of the distribution in the range of $\pm 3\sigma$ around the maximum;
- the fraction of events outside of the $\pm 3\sigma$ range around the maximum — $f_{3\sigma}$;
- the rms of the whole distribution.

All four quantities described above can be minimized by varying c_{BAC} and c_μ and they all give consistent results. This is shown in fig. 10, where contours of one standard deviation from the minimum are plotted for the four resolution estimators, for 100 GeV hadrons. The width of the distribution, as obtained from FWHM, or from the rms in the $\pm 3\sigma$ range, does not depend strongly on c_{BAC} and c_μ, as most of the events are well contained in FCAL giving no significant signal in BAC. These two quantities give thus weak constraints on c_{BAC} and c_μ. Stronger constraints are obtained when the tails of the distribution (in terms of rms for the whole distribution, or $f_{3\sigma}$) are minimized. Based on these considerations, the calibration constants c_{BAC} and c_μ are determined from the rms minimization, as this quantity is sensitive to both the width and the tails of the distribution, and gives a more reliable estimate of errors. After checking that the calibration constants do not depend substantially on the beam energy, the constants were determined in a combined analysis of the 50, 75 and 100 GeV data:

$$c_{BAC} = 0.82 \pm 0.02 \text{ GeV/ch.}$$

$$c_\mu = 0.0094 \pm 0.0003 \text{ GeV/ch.}$$

For comparison, the calibration constant for the stand-alone backing calorimeter is $c^0_{BAC} = 0.69 \pm 0.01$. The difference in the calibration constants may reflect a different composition of showers entering BAC in each case. In our previous test setup [6], the iron plates of the backing calorimeter were interleaved with plastic limited streamer tubes filled with a mixture of isobutane and argon. The calibration constant obtained in the stand-alone mode was then bigger than the one obtained in the intercalibration of the uranium and iron calorimeters. This increase of signal observed in BAC for a given energy deposit was partly attributed to the flux of neutrons originating in uranium. The effect of the neutron flux, in the case of the aluminium proportional chambers filled with a nonorganic gas, is expected to be negligible.

The correlation between the energy seen in FCAL and the leaking energy measured with the BAC calorimeter and the muon chambers, after calibration, is shown for 100 GeV in fig. 11. We have checked the linearity of the calibration by studying the fraction of measured energy missing in the calorimeters as a function of the fraction of energy deposited in BAC. The results are shown in fig. 12. We have used for this study the 50, 75 and 100 GeV hadron runs. For events with energy deposits in BAC up to 25% of the total measured energy, the linearity of our calibration is good. In about 1% of all the events (see fig. 13), those with high energy deposits in BAC, we may miss up to about 40% of the total energy. Those are events with small energy deposits in FCAL and possibly with high energy losses in the nonactive material that we are unable to account for, without destroying the linearity of our intercalibration. We cannot exclude that part of the missing energy might have escaped through the back plane of the BAC without entering into the veto calorimeter, whose lateral size is smaller than that of the BAC.

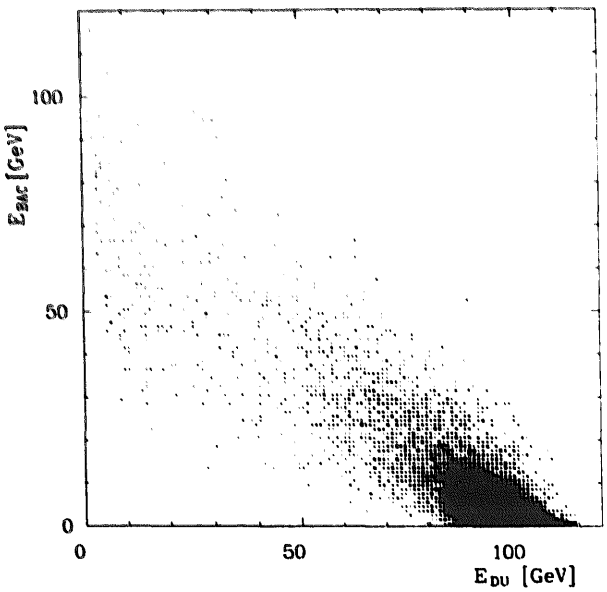

Fig. 11. Correlation between the energy measured in BAC (including μ_1 muon chambers) and the energy measured in FCAL, for a 100 GeV hadron beam.

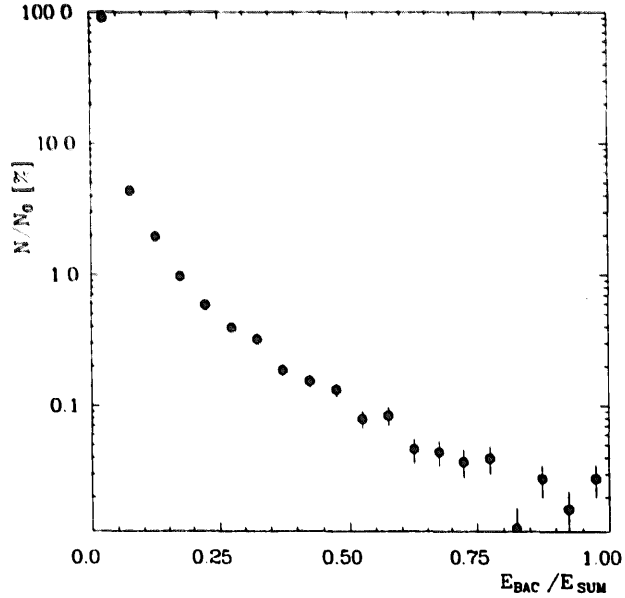

Fig. 13. Percentage of events with a given fraction of the total measured energy deposited in BAC, E_{BAC}/E_{SUM}, as a function of this fraction.

3.2. *Impact of the backing calorimeter on the total energy measurement*

We have studied the resolution of the uranium calorimeter and of the system of both calorimeters (with muon chambers included in the BAC measurement) as a function of a cut applied in the BAC prototype. The influence of this cut on the width of the distribution (in terms of σ from FWHM) is shown in fig. 14. The cut on the BAC calorimeter improves the energy resolution from $(40.8 \pm 0.3\%)/\sqrt{E}$ to $(38.1 \pm 0.3\%)/\sqrt{E}$ after rejecting about 30% of events. By adding the measured leakage (without reducing the number of events) the resolution is improved from $(40.8 \pm 0.3\%)/\sqrt{E}$ to $(39.9 \pm 0.3\%)/\sqrt{E}$. The influence of the BAC calorimeter on the energy measure-

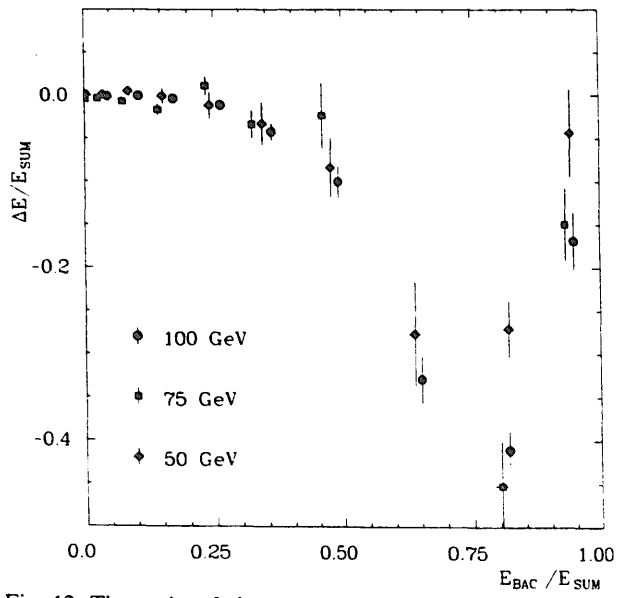

Fig. 12. The ratio of the mean energy missing in the whole calorimeter system, ΔE (determined from the nominal beam energy), to the total energy measured, E_{sum}, as a function of the fraction of energy deposited in BAC, for 50, 75 and 100 GeV hadron events, as indicated on the plot.

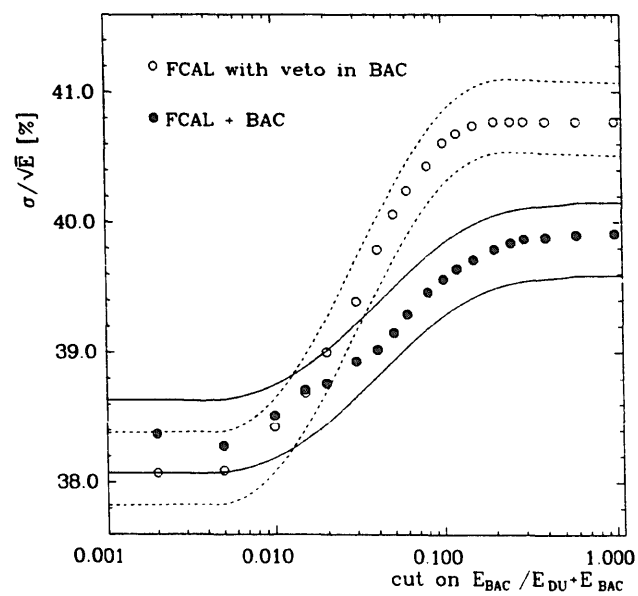

Fig. 14. The energy resolution $\sigma/\sqrt{E}$ for the FCAL prototype alone (with BAC as veto) and the combined FCAL and BAC prototypes, as a function of the cut on the fraction of energy leaking into BAC, for a 100 GeV hadron beam. The beam momentum spread is not subtracted.

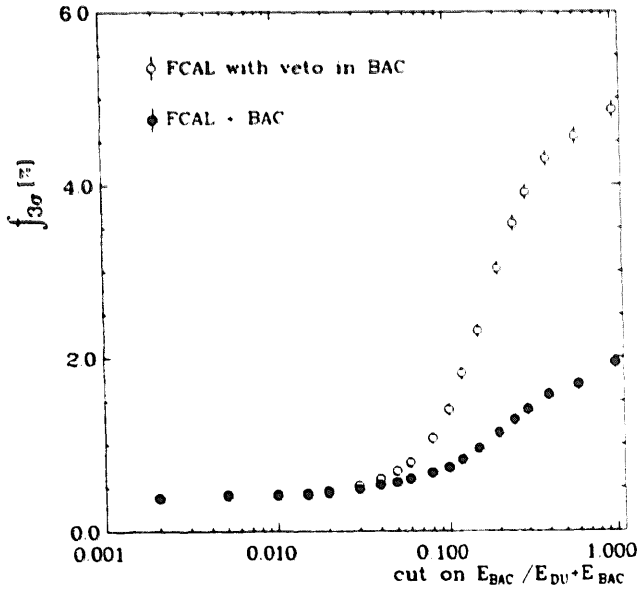

Fig. 15. The tail contents $f_{3\sigma}$, as measured for the FCAL prototype alone (with BAC as veto) and the combined FCAL and BAC prototypes, as a function of the cut on the fraction of energy leaking into BAC, for a 100 GeV hadron beam.

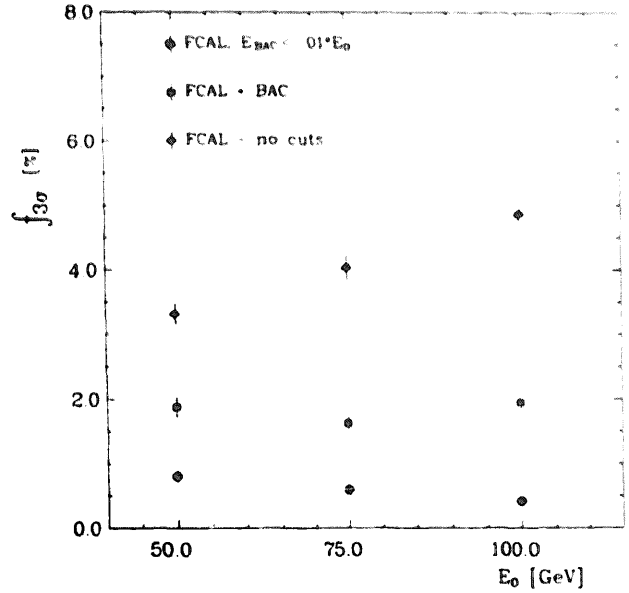

Fig. 17. The tail contents $f_{3\sigma}$ as a function of the incident beam energy E_0, for the FCAL prototype alone (with and without the leakage cut in BAC) and for the combined FCAL and BAC prototypes, as indicated in the plot.

ment is more apparent when one considers $f_{3\sigma}$. When correcting for energy leakage, the tails of the distribution are reduced from $4.86 \pm 0.12\%$ to $1.94 \pm 0.07\%$ for all events. When selecting a sample of events fully contained in the FCAL prototype, $f_{3\sigma}$ is reduced to $0.41 \pm 0.04\%$. The results on $f_{3\sigma}$ are presented in fig. 15.

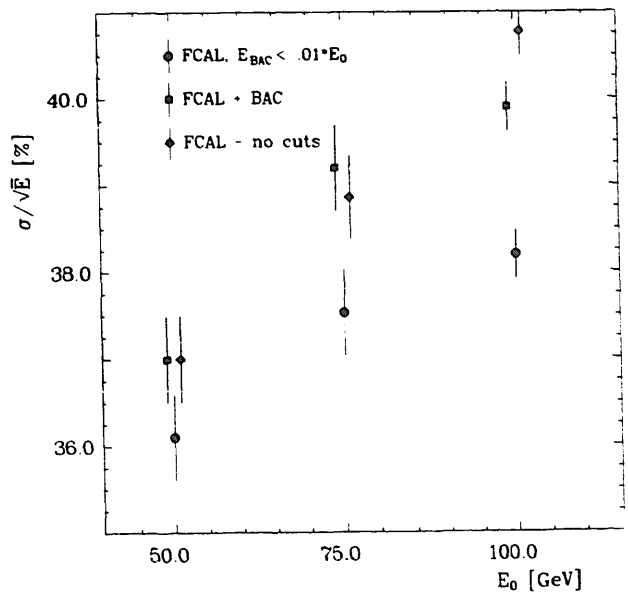

Fig. 16. The energy resolution $\sigma/\sqrt{E}$ as a function of the incident beam energy E_0, for the FCAL prototype alone (with and without the leakage cut in BAC), and for the combined FCAL and BAC prototypes, as indicated in the plot.

All results discussed above were obtained for a beam energy of 100 GeV. We have also studied the influence of BAC on the energy measurement for hadron beams of 50 and 75 GeV. The results on the resolution of energy measurement and the tails of the energy distribution, with and without cuts, for 50, 75 and 100 GeV hadron runs are summarized in figs. 16 and 17. The influence of BAC on the width of the energy distribution is not significant at 50 GeV. It becomes visible at 75 GeV, if we use the BAC prototype to reject leakages, whereas adding the BAC signal improves the resolution only at 100 GeV. The tails of the response distribution also increase with energy, when the BAC information is not used (see fig. 17). Correcting for the estimated leakage can reduce $f_{3\sigma}$ by over a factor of 2. A cut of 1% on the energy leakage into BAC can suppress $f_{3\sigma}$ to a constant level of less than 1%. From figs. 16 and 17 we may infer that the backing calorimeter will be of special importance, when measuring the high energy jets in ZEUS.

4. Conclusions

We have studied the performance of the combined prototypes of the high resolution uranium calorimeter of the ZEUS detector and a much coarser backing calorimeter. The role of the backing calorimeter is to monitor the energy leaking from the uranium calorimeter. The test results, obtained in an exposure of the calorimeter system to a hadron beam at the CERN SPS, show that the backing calorimeter does fulfil its

role very well. The measurement of the leaking energy is feasible, if only the calibration of the BAC calorimeter is corrected with respect to the stand-alone one. Also the muon chambers located between the two calorimeters can be used to improve the energy measurement through better estimation of energy losses in a nonactive material behind the uranium calorimeter. It was verified that the intercalibration of the two calorimeters does not depend on the beam energy and is linear for energy deposits in the backing calorimeter up to about 25% of the total energy. The backing calorimeter can be used either to select a high resolution sample of events fully contained in the uranium calorimeter, or to correct for leakage by adding the signals. In both cases the energy measurement is improved.

Acknowledgements

We would like to thank the members of the ZEUS collaboration, in particular our colleagues from the Calorimeter Group for their support in building our test setup at CERN, and for many useful discussions. Special thanks are due to R. Dąbrowski, W. Dominik D. Genser, M. Hamela, Z. Mazur and technicians from Warsaw University for building the BAC chambers. We also thank K. Jelen for many advices and help in preparing the tests as well as W. Filipek for his work on assembling the BAC detector at CERN.

We appreciate the hospitality and excellent technical support we have received at CERN, where the measurements have been performed. This work would have not been possible without the financial support from DESY.

References

[1] ZEUS, a detector for HERA, letter of intent, DESY (June 1985); The ZEUS detector, technical proposal, DESY (March 1986); The ZEUS detector, status report 1989, DESY (March 1989).
[2] Technical proposal for the H1 Detector, DESY (1986); Technical progress Report, H1 Detector, DESY (1987).
[3] U. Behrens et al., Nucl. Instr. and Meth. A289 (1990) 115.
[4] H. Abramowicz et al., ZEUS Note 90-091, ZEUS Note 90-099, to be published.
[5] J. Krüger, DESY 90-163.
[6] I. Kudla et al., Nucl. Instr. and Meth. A300 (1991) 480.